Quantum suppression of collisional loss rates in optical traps

H. M. J. M. Boesten, B. J. Verhaar, and E. Tiesinga
Department of Physics, Eindhoven University of Technology, P.O. Box 513, 5600 MB Eindhoven, The Netherlands
(Received 30 March 1993)

We present a coupled-channel study of optical collisions, restricted to a single atom-laser manifold. Outside of a resonance region around the Condon point, we find a simple representation of the solution in terms of propagating complex dressed states. The probability flux for the $^2P_{3/2}+S$ state at small interatomic distances can be interpreted in terms of two such interfering dressed states. The coupled-channel solution displays some features that have previously been obtained with semiclassical optical-Bloch-equation methods. An important quantum effect, however, is a strong reduction of atom loss rates at low collision energies that is roughly proportional to E^{-2}.

PACS number(s): 32.80.Pj, 42.50.Vk

I. INTRODUCTION

In recent years a rapid development has taken place in the field of cooling atomic gases and storing them in optical and magnetic traps. The interest is stimulated by exciting opportunities offered by such cold gases, such as the possible realization of Bose-Einstein condensation and precision experiments such as the construction of an ultrastable Cs clock. The interest also comes from the expectation that collisions between atoms proceed in an unusual way at the temperatures which are now being achieved. At low temperatures, the collision between a ground-state atom and an optically excited atom proceeds differently due to the fact that the spontaneous-emission time becomes comparable with the collision time, which makes it essential to include spontaneous emission in a more fundamental way in the description of the collision (for an overview of research in this area, see Julienne, Smith, and Burnett [1]).

A crucial aspect determining to a great extent the possibilities of carrying out experiments on atoms in traps is the existence of loss mechanisms which shorten the half-life of the atom density. For (magneto-)optical traps Gallagher and Pritchard [2] first pointed to the existence of two important mechanisms, both of which occur in atom-atom collisions. The basic process involved is resonant laser excitation

$$A(S)+A(S)+\hbar\omega \rightarrow A(^2P_{3/2})+A(S) \qquad (1)$$

at large interatomic distance and subsequent acceleration along a $-C_3/R^3$ attractive excited-state-potential surface. This is followed by either spontaneous emission and the possibility of a subsequent escape of the fast-moving ground-state atoms, or, more importantly, by an exothermal fine-structure transition $^2P_{3/2} \rightarrow {}^2P_{1/2}$ at close interatomic distance giving the atoms enough energy to escape.

After the basic description by Gallagher and Pritchard the theory was further developed in two papers [3,4], which clearly demonstrated the rich variety of physical phenomena involved in optical collisions. In these papers the atomic motion was treated classically, which introduces an ambiguity as to the choice of the relative atomic velocity on the excited potential. This type of ambiguity can be avoided in a purely quantum-mechanical theory. It is clear, however, that a rigorous fully quantum-mechanical theory of optical collisions is beyond present computational possibilities. Therefore it is of interest to investigate partial aspects of the full problem in order to obtain so much insight that adequate approximative descriptions can eventually be developed. One such study was recently carried out in the nonsaturated regime on the basis of the WKB and a stationary-phase-like approximation for the atomic motion [5]. The result was written in the form of a product of an absorption line shape and a survival probability on the excited potential with an excited-state velocity determined by energy conservation.

In this paper the treatment will be fully quantum mechanical, but limited to a single manifold [6] of coupled states $|e,N\rangle$ and $|g,N+1\rangle$ of the combined molecule-laser system and a single combination of relative orbital angular momentum quantum numbers l' and l for the excited and unexcited two-atom system, respectively. Here e and g denote optically coupled excited and unexcited internal states of the combined two-atom system, while N and $N+1$ stand for the associated numbers of laser photons.

II. METHOD OF CALCULATION

For the sake of definiteness we concentrate on the optical collision of Cs atoms, and on the 0_u^+ and 0_g^+ excited and ground states, respectively [3,5]. We thus deal with a simple two-channel model of an optical collision, but believe that the conclusions shed light on more realistic situations with complications such as a number of subsequent radial avoided crossings due to hyperfine structure or a number of excited potential curves besides 0_u^+. We consider collision energies from the mK range down to values around 10 μK, where recoil effects can still be neglected both for linear and angular momentum. In view

of the predominance of the $-C_3/R^3$ potential, the centrifugal effects in the e channel do not depend on the precise value of l', which may therefore be taken equal to l.

The above restriction to a single manifold allows us to take into account the loss of probability flux due to spontaneous emission but we do not consider the "recycling" of ground-state atoms thereby produced on the next lower manifold, i.e., their subsequent laser excitation. This first-order treatment in the spontaneous-emission rate is valid as long as the depletion of the original manifold is small. In practice, this also implies a small depletion of the ground state, i.e., a restriction to the unsaturated regime. The implied near-linear intensity dependence is indeed indicated by experimental data of Sesko *et al.* [7] and is also reproduced by optical Bloch equation calculations [4]. Also for the more general case, where the depletion of the original manifold is not small, the present single-manifold study is of interest, since the waves generated in lower-N manifolds by spontaneous emission again behave according to the same coupled-channel equations, so that the properties of the solution may be used to develop an approach for the total problem.

We thus solve the system of coupled radial equations

$$\left[-\frac{\hbar^2}{2\mu}\frac{d^2}{dR^2}+\frac{\hbar^2 l(l+1)}{2\mu R^2}+\hbar\,\underline{\underline{\omega}}(R)\right]\underline{F}(R)=E\,\underline{F}(R), \tag{2}$$

with μ the reduced mass and

$$\underline{F}(R)=\begin{pmatrix}F_e(R)\\F_g(R)\end{pmatrix} \tag{3}$$

the coupled radial wave functions associated with the $|e,N\rangle$ and $|g,N+1\rangle$ states. Furthermore,

$$\underline{\underline{\omega}}(R)=\begin{pmatrix}-\Delta(R)-i\Gamma & \frac{1}{2}\Omega_r\\ \frac{1}{2}\Omega_r & 0\end{pmatrix}, \tag{4}$$

in which $\Delta(R)=\Delta(1-R_C^3/R^3)$ is the local laser detuning with R_C the Condon point. For simplicity we neglect the long-range retardation and the $1/R^6$ van der Waals potential at the large distances involved, while the spontaneous-emission rate $\Gamma = 32.7\times10^6\ \mathrm{s}^{-1}$ and the Rabi frequency Ω_r are taken independent of R [4,5]. Including R-dependent corrections in our coupled-channel calculations is straightforward but is not expected to change the basic conclusions. We solve the set of coupled equations (2), subject to boundary conditions to be specified below.

It turns out that our coupled-channel solution has a simple behavior outside the resonance region around R_C. It can be described to a very good approximation in terms of decoupled solutions in a local-R basis of complex dressed states consisting of the eigenvectors of the non-Hermitian matrix $\underline{\underline{\omega}}$:

$$\begin{aligned}|1(N)\rangle &= \cos(\theta)|e,N\rangle+\sin(\theta)|g,N+1\rangle,\\ |2(N)\rangle &= -\sin(\theta)|e,N\rangle+\cos(\theta)|g,N+1\rangle\end{aligned} \tag{5}$$

with complex coefficients determined by $\tan(2\theta)=-\Omega_r/[\Delta(R)+i\Gamma]$ and the complex eigenvalues $-\frac{1}{2}\hbar[\Delta(R)+i\Gamma]\pm\frac{1}{2}\hbar\Omega(R)$ in which $\Omega(R)=\{\Omega_r^2+[\Delta(R)+i\Gamma]^2\}^{1/2}$, the sign of the square root being chosen in such a way that $\mathrm{Re}[\Omega(R)]$ is positive right of R_C. The associated damped radial wave functions $F_{i(N)}(R)$ satisfy the equations

$$\left[-\frac{\hbar^2}{2\mu}\frac{d^2}{dR^2}+\frac{\hbar^2 l(l+1)}{2\mu R^2}-\frac{1}{2}\hbar[\Delta(R)+i\Gamma]\pm\frac{1}{2}\hbar\Omega(R)\right]F_{i(N)}(R)=EF_{i(N)}(R) \tag{6}$$

with the + or − sign for $i=1$ or 2.

In terms of the above decoupled solutions the boundary conditions for the collision problem are an incoming $|2(N)\rangle$ wave right of R_C and $|1(N)\rangle,|2(N)\rangle$ waves leaving the environment of R_C both to the left and right. For the collision energy E less than the threshold energy $\mathrm{E_{th}}=-\frac{1}{2}\hbar\Delta+\frac{1}{2}\hbar\,\mathrm{Re}[\Omega(\infty)]$ the $|1(N)\rangle$ radial wave function should go to 0 as $R\to\infty$. Our main conclusions remain valid for other boundary conditions, in particular for waves approaching R_C from the direction of the origin and thus also for the coupled problem where the reflection of radially ingoing waves from the small-R region calculated in Ref. 3 is taken into account. For the simple case without spontaneous emission ($\Gamma=0$, $\mathrm{E}_{i(N)}$ real) the boundary conditions are illustrated in Fig. 1. We solve the set of complex coupled equations (2) in the uncoupled basis in the resonance region around R_C with a width of a few hundred a_0 to find a set of linearly independent coupled basis solutions. Subsequently, we form a linear combination to satisfy the above conditions at the boundaries of this region.

In the first instance we restrict ourselves to $l=0$. The program has been checked by applying it to a simple model in which the actual $-C_3/R^3$ potential is replaced by a rectilinear potential having the same derivative at R_C. For such a simple avoided crossing analytical ex-

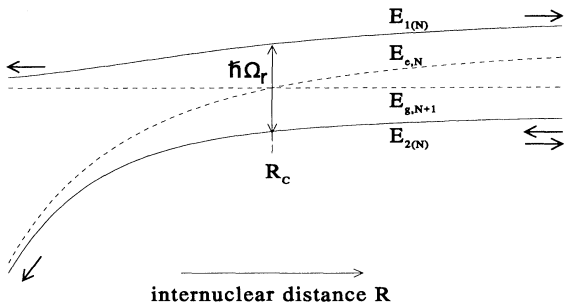

FIG. 1. Boundary conditions for collision problem ($\Gamma=0$): an incoming wave in the $|2(N)\rangle$-channel right of R_C and outgoing waves in all channels.

pressions for reflection and transmission coefficients can be derived [8] which agree excellently with our numerical results.

III. RESULTS AND DISCUSSION

Figure 2 shows the probability fluxes J_g, J_e, and their sum in the uncoupled basis, following from the coupled-channel solution for initial kinetic energy $E = 1$ mK, detuning $\Delta = -\Gamma$, and Rabi frequency $\Omega_r = 0.8\Gamma$. For reasons to be explained below we normalize to $J_g + J_e = 1$ at small R. We see a behavior with an interesting physical interpretation: a decreasing J_g at large R due to laser excitation on approaching $R_C = 2950a_0$, an excited-state flux J_e starting at somewhat lower values, then first decreasing slowly due to the combined effect of laser excitation and spontaneous emission and subsequently, after the passage of the resonance region around R_C, decaying more rapidly due to disappearing laser excitation. Around $2000a_0$, J_g (as well as $J_g + J_e$) reaches a plateau, with Rabi oscillations in antiphase in J_e and J_g. It turns out that in all our $l = 0$ calculations the passage through the avoided crossing leads to negligible reflection of waves back to large R. This applies even to the lowest collision energies considered. This is in agreement with Ovchinnikova's analytical results [8] for rectilinear crossing potentials, which can be readily extended to the present calculations including spontaneous emission, as we will show elsewhere. It also turns out that the Rabi oscillations do not appear in the sum $J_g + J_e$, in agreement with classical expectations. The decrease of $J_g + J_e$ right of the plateau is due to the loss of probability flux from the considered manifold by spontaneous emission. In principle, one would have to go to the next lower manifold in order to follow the recycling of this incoherent part of the scattering state.

It turns out that the oscillating J_e pattern is in its totality rather accurately proportional to Ω_r^2, within wide intensity limits to be given below, provided the solution is normalized to a prescribed value for the total atom flux $J_g + J_e$ in the region left of R_C where this sum has reached a constant plateau. Figure 3 shows the J_e pattern for $\Omega_r = 0.4\Gamma$, i.e., for one-fourth of the original intensity. Clearly, apart from a nonlinear interval around R_C, the J_e pattern is simply shifted along the logarithmic axis relative to that in Fig. 2.

The linear intensity dependence can be explained in the same way that the absence of saturation in the experimental Cs loss rate of Ref. [7] is explained in Ref. [1]: in the plateau region most of the excited-state amplitude is due to off-resonant excitation occurring well inside R_C, as this process is favored by improved survival. The flux lost previously to the lower manifold by spontaneous emission is recycled according to the same off-resonant excitation probability. In this respect it is of importance that the atomic velocity increase after the first excitation–spontaneous-emission cycle is still rather low. The new J_g, J_e combination on the next lower manifold is therefore expected to be proportional to that of the original manifold and can consequently be considered to be part of the same total pure state, for which J_g and J_e behave in the plateau region as given in Fig. 2.

On the basis of this near linearity it is the ratio J_e/Ω_r^2 that in the limit $\Omega_r \to 0$ is relevant for the comparison

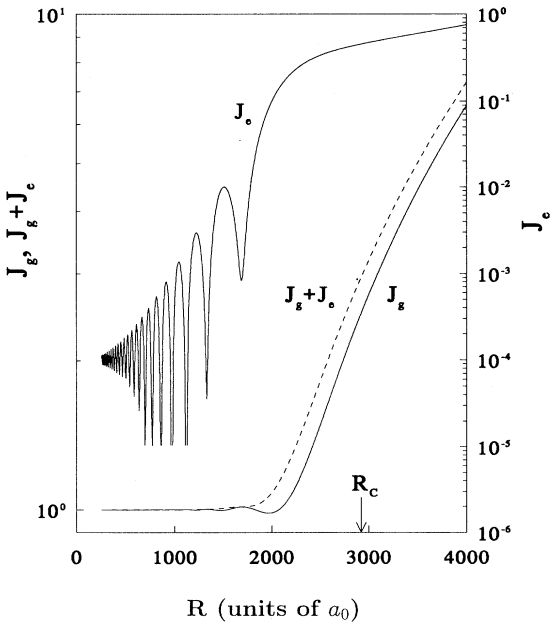

FIG. 2. Probability fluxes J_g, $J_g + J_e$ (left scale), and J_e (right scale) in uncoupled basis as a function of internuclear distance, following from coupled-channel calculations for $E = 1$ mK, $\Delta = -\Gamma$, and $\Omega_r = 0.8\Gamma$.

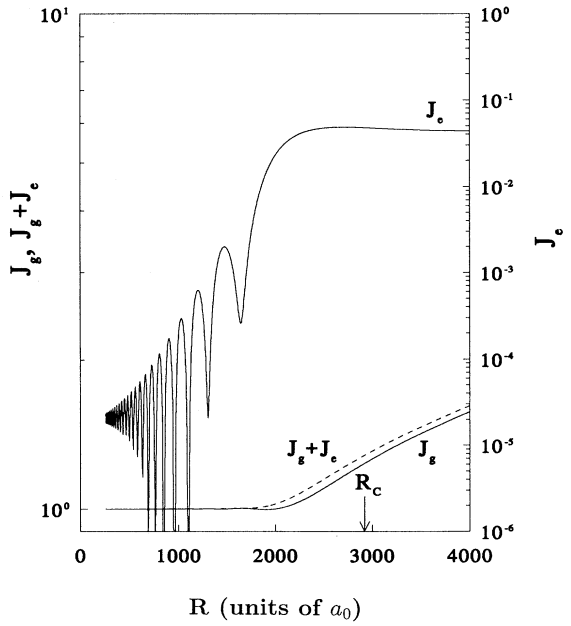

FIG. 3. Fluxes J_g, $J_g + J_e$ (left scale), and J_e (right scale) in uncoupled basis, following from coupled-channel calculations for $E = 1$ mK, $\Delta = -\Gamma$, and $\Omega_r = 0.4\Gamma$.

with experiment. Then normalization with respect to the plateau value of $J_g + J_e$ is completely equivalent to normalization relative to the incident value of $J_g + J_e$, since the sum does not change near R_C in this limit. Figure 4 shows the functions J_e/Ω_r^2, J_g, and $J_g + J_e$ in the zero-intensity limit for $\Delta = -\Gamma$ and $E = 1$ mK. We now see a maximum of the excited-state flux near R_C. To illustrate the accuracy of the theoretical linear intensity dependence of our J_e we give in Fig. 5 the value of J_e at $R = 10a_0$ as a function of $(\Omega_r/\Gamma)^2$ for $E = 1$ mK and $\Delta = -\Gamma$. Clearly, the linear dependence is very accurate until $\Omega_r/\Gamma = 0.6$.

It turns out that the period of the Rabi oscillations in Figs. 2 and 3 agrees rather precisely with the local precession frequency $\Omega_{\text{eff}}(R) = \{\Delta^2(R) + \Omega_r^2\}^{1/2}$ if one assumes the effective velocity to be the average $\{v_g + v_e(R)\}/2$ of the velocities on the g and e potentials. Another interesting feature can also be seen, for instance, in Fig. 2. The oscillation is seen to be sharper at the bottom than at the top. This can be explained classically in terms of the fact that part of the population oscillates between the g and e states. The instantaneous velocity therefore oscillates between the values v_g and v_e of the local velocities.

Similar properties are obtained at lower energies. In Fig. 6 we show as an example the radial fluxes for $E = 10$ μK and $\Delta = -\Gamma$. In general, for the same detuning and intensity the main J_e/Ω_r^2 maximum increases with decreasing energies, corresponding to the slower motion of the atoms through the resonance region, with the associated more effective excitation. Other features seen for lower energies are a smaller amplitude of the Rabi oscillations, arising from a better adiabatic following of the polarization vector. The much stronger damping of J_e left of R_C is discussed below.

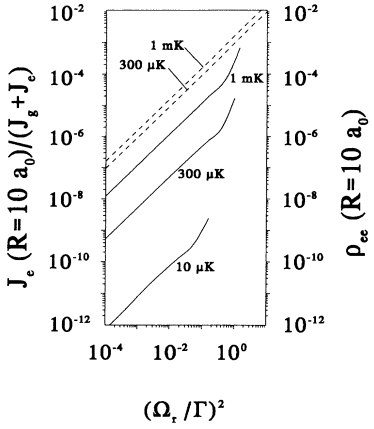

FIG. 5. Normalized flux J_e (solid lines) and ρ_{ee} (dashed lines), obtained with OBE, at $R = 10a_0$ as a function of $(\Omega_r/\Gamma)^2$ for some selected energies and $\Delta = -\Gamma$, illustrating near-linear intensity dependence.

In Fig. 5 we have also presented the intensity dependence of J_e at $R = 10a_0$ for $E = 300$ μK and $E = 10$ μK. We notice that the linearity of J_e persists to lower maximum intensities for decreasing energies, again corresponding to more effective laser excitation.

The J_e pattern in the foregoing Figs. 2 and 3 can be understood more in detail in terms of the interference of two radial waves in the complex dressed-state basis $|1(N)\rangle$ and $|2(N)\rangle$. For an intuitive picture of these radial waves it is useful to calculate the radial fluxes in

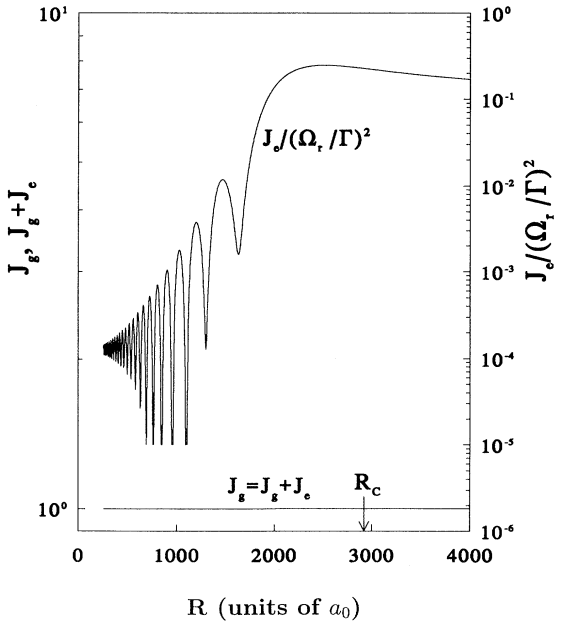

FIG. 4. Fluxes J_g, $J_g + J_e$, and $J_e/(\Omega_r/\Gamma)^2$ in the zero-intensity limit for $E = 1$ mK and $\Delta = -\Gamma$.

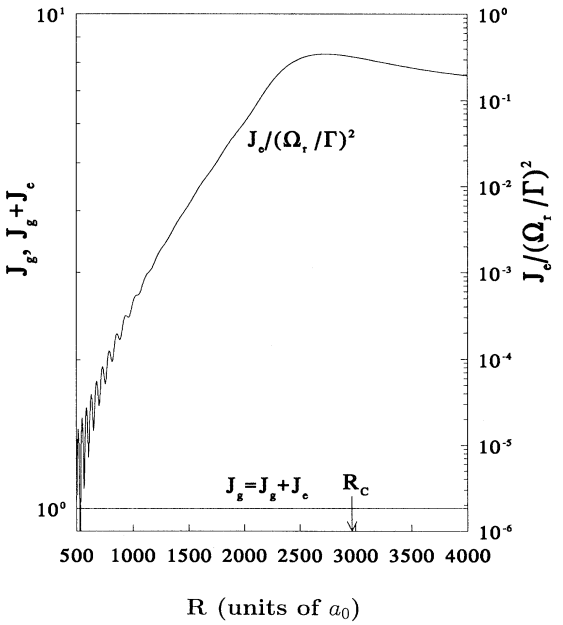

FIG. 6. Fluxes J_g, $J_g + J_e$, and $J_e/(\Omega_r/\Gamma)^2$ in the zero-intensity limit for $E = 10$ μK and $\Delta = -\Gamma$.

this (nonorthogonal) basis. Figure 7 shows $J_{1(N)}$ and $J_{2(N)}$ as functions of R for $E = 1$ mK, $\Delta = -\Gamma$, and $\Omega_r = 0.4\Gamma$. The flux $J_{1(N)}$ starts from zero right of R_C, in agreement with the boundary conditions in Fig. 1. Near R_C, $J_{1(N)}$ increases strongly and reaches a maximum $600a_0$ left of R_C. For all interatomic distances, however, $J_{1(N)}$ is much smaller than $J_{2(N)}$. Although $J_{1(N)}$ still shows some remnants of a Rabi-type oscillation it is much smoother than J_e. A similar remark applies to $J_{2(N)}$ compared to J_g. This already illustrates that the complex dressed states are a suitable basis to obtain radial waves with as regular behavior as possible. It is also confirmed by the behavior which develops starting at the plateau region towards smaller distances: the $1(N)$ and $2(N)$ components of the coupled channel solution turn out to be uncoupled exponentially damped waves converging to $R = 0$, with regularly changing complex wave numbers. A simple calculation based on such locally exponential waves shows that the amplitude of the strongly oscillating J_e pattern is roughly equal to $[J_{1(N)}J_{2(N)}]^{1/2}(\hbar\Omega_r/2)(\hbar\Delta)^{-3/4}E^{-1/4}(R/R_C)^{9/4}$. On the other hand, we find the oscillations to take place around an average value equal to $\cos^2(\theta)J_{1(N)} + \sin^2(\theta)J_{2(N)}$, which tends to $J_{1(N)}$ near $R = 10a_0$. Both predictions are confirmed by the actual J_e patterns.

We thus find that $J_{1(N)}$ is the physically interesting quantity for the fine-structure changing loss rate, since it is equal to the flux J_e of excited atoms at the corresponding avoided crossing near $10a_0$. The $J_{2(N)}$ flux determines the radiative escape loss, because its contribution to J_e dominates in the wider range of interatomic distances where radiative escape is most probable as the final fate of the atoms.

For the physical interpretation of our coupled-channel solutions it is of importance to compare $J_{1(N)}$ and $J_{2(N)}$ with uncoupled adiabatic solutions $J^0_{1(N)}$ and $J^0_{2(N)}$. This will make clear to which radial region the nonadiabatic excitation is confined. Figure 8 shows $J_{1(N)}/J^0_{1(N)}$ and $J_{2(N)}/J^0_{2(N)}$ for $E = 10$ μK, $\Delta = -\Gamma$, and $\Omega_r = 0.2\Gamma$. The uncoupled fluxes are normalized in such a way that the two ratios tend to 1 for $R \to 0$. Clearly, most of the excitation of $J_{1(N)}$ occurs left of R_C due to the finite radial velocity. For the same reason the ratio $J_{2(N)}/J^0_{2(N)}$ grows for decreasing R: the $2(N)$ dressed state is depleted more slowly than for zero velocity.

At this point we make a comparison with treatments based on the optical-Bloch-equation (OBE) method [4]. In Fig. 5 we compare our J_e flux at $R = 10a_0$ for $\Delta = -\Gamma$, normalized as above, to the OBE value of the excited-state population ρ_{ee} at the same radius. For higher energies, not shown in the figure, where the radial motion can be treated classically, these quantities are equal. For the 1-mK and 300-μK OBE calculations we used the "energy conserving" trajectory choice [5]. For lower collision energies, below E_{th}, we adopted the "switched" and "asymptotic" trajectory choices, which lead to almost identical results (within 15%). We find a suppression of the excited-state occupation probability, due to the quantum-mechanical nature of the radial motion, by about one order of magnitude already at 1 mK and increasing strongly with decreasing energy, roughly proportional to E^{-2}.

The origin of this tremendous suppression is the destructive interference of the radial waves on the excited

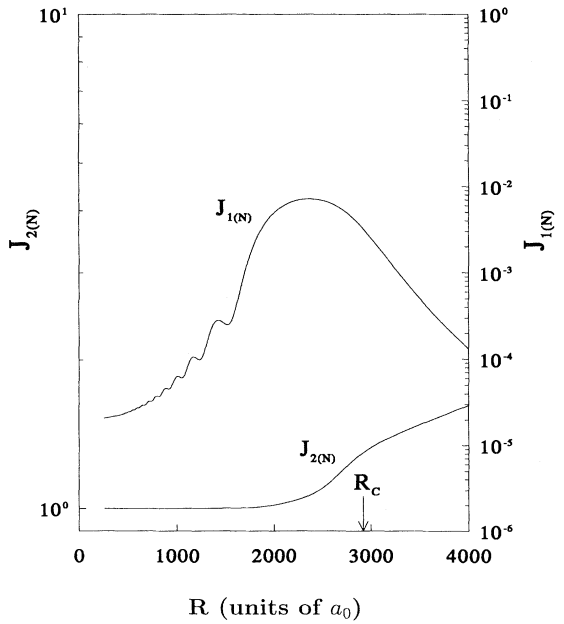

FIG. 7. Dressed-state fluxes $J_{2(N)}$ (left scale) and $J_{1(N)}$ (right scale) in coupled basis for $E = 1$ mK, $\Delta = -\Gamma$, and $\Omega_r = 0.4\Gamma$.

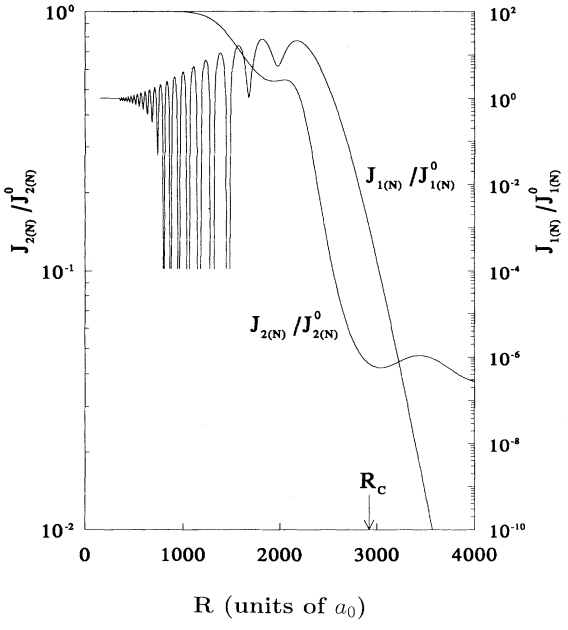

FIG. 8. Ratios $J_{1(N)}/J^0_{1(N)}$ (left scale) and $J_{2(N)}/J^0_{2(N)}$ (right scale) of fluxes in dressed-state basis and adiabatic fluxes as a function of R for $E = 10$ μK, $\Delta = -\Gamma$, and $\Omega_r = 0.2\Gamma$.

potential, arising from excitation at the various radii left of R_C. Adding these wavelets as they arrive for instance at $10a_0$, their phase difference is larger for lower collision energies: the velocity increase along the excited-state potential during the passage through the excitation region becomes more and more important compared to the initial velocity. This destructive interference is fully taken into account in our approach and is left out in a classical treatment of radial motion. Apparently, it is a dominating quantum effect at low collision energies. The experimental relevance is associated with a strongly reduced atom loss in the unsatured regime, both for the fine-structure and rediative-escape loss mechanisms.

All previous results were restricted to $l = 0$. In order to get an impression of the influence of centrifugal effects, we concentrate on a single l value equal to $kR_C/2$, with k the asymptotic wave number, and solve the coupled equations. Far left of R_C we include the reflection from the centrifugal barrier in the $2(N)$ channel and normalize with respect to the flux of the left-going wave.

Again we find a linear intensity dependence of the J_e pattern. This is illustrated in Fig. 9, where we present the probability flux J_e at $R = 10a_0$ as a function of $(\Omega_r/\Gamma)^2$ for $E = 300$ μK, $\Delta = -\Gamma$, and $l = 30$. We see a linear behavior up to $\Omega_r/\Gamma = 0.6$ in agreement with the previously mentioned off-resonant excitation. Comparing J_e in Fig. 9 with J_e in Fig. 5 for $l = 0$, we note that the survival rate is about one order of magnitude lower at $l = kR_C/2$. Again, we compare also with the OBE survival. Apparently, the quantum suppression is now even larger than for $l = 0$. This may be ascribed to the lower local radial velocity v_g, taking into account the centrifugal barrier, which leads to an increased destructive interference.

Our calculations thus show that higher l and lower E survival rates are strongly suppressed relative to OBE values. It should be noted that in our coupled-channel calculations the unsaturated domain is restricted to much lower intensities than suggested for instance by the Rb experiments in Refs. [7,9]. This is probably due to the fact that the inclusion of nuclear spin leads to a considerable reduction of Rabi frequencies Ω_r, the total optical dipole strength being distributed over the individual anticrossings with the various $^2P_{3/2} + S$ hyperfine states. We are developing the computational scheme for the inclusion of hyperfine structure both in the $S + S$ and the $^2P_{3/2} + S$ channels, needed for the description of such optical collisions.

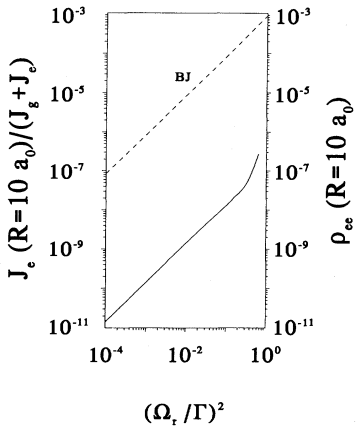

FIG. 9. Normalized flux J_e (solid line) and ρ_{ee} (dashed line), obtained with OBE, at $R = 10a_0$ as a function of $(\Omega_r/\Gamma)^2$ for $E = 300$ μK, $\Delta = -\Gamma$, and $l = 30$.

[1] P.S. Julienne, A.M. Smith, and K. Burnett, in *Advances in Atomic, Molecular and Optical Physics*, edited by D.R. Bates and B. Bederson (Academic, San Diego, CA, 1993), p. 141.
[2] A. Gallagher and D.E. Pritchard, Phys. Rev. Lett. **63**, 957 (1989).
[3] P.S. Julienne and J. Vigué, Phys. Rev. A **44**, 4464 (1991).
[4] Y.B. Band and P.S. Julienne, Phys. Rev. A **46**, 330 (1992).
[5] A.M. Smith, K. Burnett, and P.S. Julienne, Phys. Rev. A **46**, 4091 (1992).
[6] C. Cohen-Tannoudji, J. Dupont-Roc, and G. Grynberg, *Atom-Photon Interactions* (Wiley, New York, 1992).
[7] D. Sesko, T. Walker, C. Monroe, A. Gallagher, and C. Wieman, Phys. Rev. Lett. **63**, 961 (1989).
[8] M. Ya. Ovchinnikova, Opt. Spektrosk. **17**, 821 (1964) [Opt. Spectrosc. (USSR) **17**, 447 (1964)].
[9] P. Feng, D. Hoffmann, and T. Walker (unpublished).